Biochimica et Biophysica Acta 1812 (2011) 1522–1531

Contents lists available at ScienceDirect

Biochimica et Biophysica Acta

journal homepage: www.elsevier.com/locate/bbadis

The nuclear receptor FXR regulates hepatic transport and metabolism of glutamine and glutamate

Barbara Renga [a,*], Andrea Mencarelli [a], Sabrina Cipriani [a], Claudio D'Amore [a], Angela Zampella [b], Maria Chiara Monti [c], Eleonora Distrutti [d], Stefano Fiorucci [a,d]

[a] Dipartimento di Medicina Clinica e Sperimentale, Università degli Studi di Perugia, Perugia, Italy
[b] Dipartimento di Chimica delle Sostanze Naturali, Università di Napoli Federico II, Napoli, Italy
[c] Dipartimento di Scienze Farmaceutiche e Biomediche, Università di Salerno, via Ponte don Melillo, Fisciano, Italy
[d] Ospedale S. Maria della Misericordia, S. Andrea delle Fratte, Perugia, Italy

ARTICLE INFO

Article history:
Received 16 May 2011
Received in revised form 21 June 2011
Accepted 23 June 2011
Available online 1 July 2011

Keywords:
Glutamine
Glutamate
Urea cycle
NAGS
FXR
Hyperammonemia

ABSTRACT

Hepatic transport and metabolism of glutamate and glutamine are regulated by intervention of several proteins. Glutamine is taken up by periportal hepatocytes and is the major source of ammonia for urea synthesis and glutamate for N-acetylglutamate (NAG) synthesis, which is catalyzed by the N-acetylglutamate synthase (NAGS). Glutamate is taken up by perivenous hepatocytes and is the main source for the synthesis of glutamine, catalyzed by glutamine synthase (GS). Accumulation of glutamate and ammonia is a common feature of chronic liver failure, but mechanism that leads to failure of the urea cycle in this setting is unknown. The Farnesoid X Receptor (FXR) is a bile acid sensor in hepatocytes. Here, we have investigated its role in the regulation of the metabolism of both glutamine and glutamate. *In vitro* studies in primary cultures of hepatocytes from wild type and $FXR^{-/-}$ mice and HepG2 cells, and *in vivo* studies, in $FXR^{-/-}$ mice as well as in a rodent model of hepatic liver failure induced by carbon tetrachloride (CCl_4), demonstrate a role for FXR in regulating this metabolism. Further on, promoter analysis studies demonstrate that both human and mouse NAGS promoters contain a putative FXRE, an ER8 sequence. EMSA, ChIP and luciferase experiments carried out to investigate the functionality of this sequence demonstrate that FXR is essential to induce the expression of NAGS. In conclusion, FXR activation regulates glutamine and glutamate metabolism and FXR ligands might have utility in the treatment of hyperammonemia states.

© 2011 Elsevier B.V. All rights reserved.

1. Introduction

The amino acids glutamine and glutamate participate in multiple biochemical pathways and are at the center of hepatic amino acid metabolism [1,2]. In the liver (Fig. 1), glutamine is transported into periportal hepatocytes by the solute carrier (SLC)-1A5 (also named ASCT2) [2,3] and is used to synthesize glutamate. This reaction is catalyzed by the enzyme glutaminase (GLS). Then, glutamate can be converted to N-acetylglutamate (NAG) by the activity of the enzyme NAG synthetase (NAGS) [4,5]. NAG is an obligatory co-activator of carbamoyl phosphate synthetase-I (CPS-I), the rate limiting enzyme in the urea synthesis (5). Alternatively, glutamate can be converted into α-ketoglutarate (αKG) on a reaction that produces ammonia, catalyzed by the enzyme glutamate dehydrogenase (GDH) [6]. In perivenous hepatocytes, the site of hepatic glutamine synthetase (GS) activity, glutamate is taken up by the transporters SLC1A2 (also named EAAT2) and SLC1A4 (also named ASCT1) and is primarily used to synthesize glutamine [7].

Farnesoid X Receptor (FXR) is a member of nuclear receptor superfamily initially characterized in the liver for its ability to regulate genes involved in bile acid synthesis and cholesterol metabolism, detoxification and excretion [8,9]. In addition, FXR plays a role in regulating genes involved in lipid metabolism, inflammatory response as well as in insulin regulated pathways [10–12]. FXR regulates gene transcription as a heterodimer with the *9-cis* retinoic acid receptor (RXR) by binding DNA responsive elements (FXREs) composed by an inverted repeat of the sequence AGGTCA (*consensus*) separated by one nucleotide (IR-1), a direct repeat sequence separated by one nucleotide (DR-1) or an everted repeat sequence separated by eight nucleotides (ER-8) [13]. Bile acids, the steroid end-products of the cholesterol metabolism, are FXR ligands: in particular FXR is strongly activated by the primary bile acid chenodeoxycholic acid (CDCA) with an EC_{50} of ≈10 μmol/L [10]. In a recent work it has been demonstrated that FXR is directly involved in the transcription of the glutamine transporter ASCT2 in HepG2 as an IR-1 sequence was found in the promoter of the human ASCT2 gene [14]. However it is unknown whether bile acids

* Corresponding author at: Dipartimento di Medicina Clinica e Sperimentale, University degli Studi di Perugia, Via E. dal Pozzo, 06122 Perugia, Italy. Tel./fax: +39 0755855819.
E-mail address: barbara.renga@unipg.it (B. Renga).

0925-4439/$ – see front matter © 2011 Elsevier B.V. All rights reserved.
doi:10.1016/j.bbadis.2011.06.009

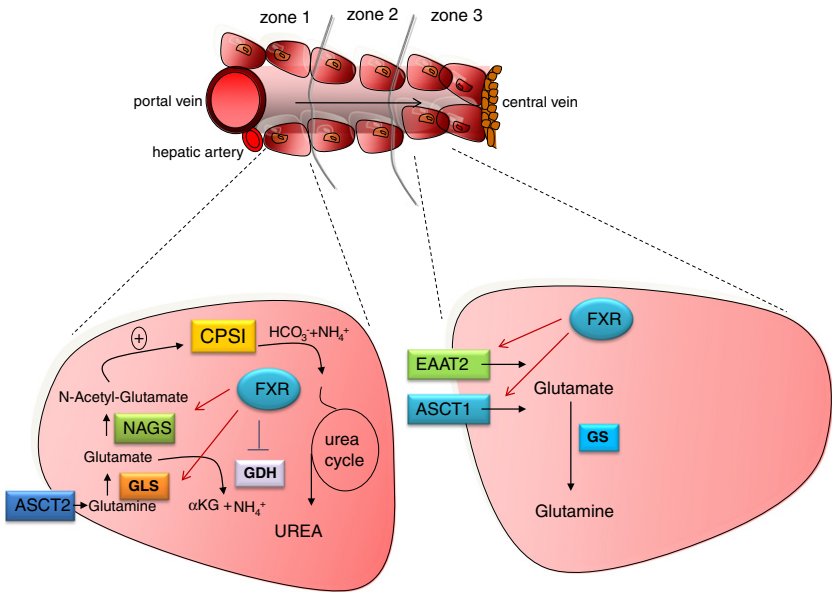

Fig. 1. Diagrammatic representation of glutamine and glutamate metabolism associated with urea cycle across the liver sinusoid. NAGS: N-acetylglutamate synthase; GDH: Glutamate dehydrogenase; CPSI: Carbamyl−phosphate-synthase-I; ASCT1: solute carrier family 1 member 5; EAAT2: solute carrier family 1 member 2; ASCT2: solute carrier family 1 member 4; GLS: Glutaminase; GS: Glutamine synthase; FXR: Farnesoid X receptor.

provide regulatory signals on genes mediating the glutamine and glutamate metabolism.

In the present study we provide the first evidence that FXR is a direct regulator of genes involved in glutamine/glutamate metabolism. More specifically, we show that the NAGS promoter contains an FXRE, an ER-8 sequence (TGAGCT*CAGGCAAC*AGGACA), whose mutation abrogates the ability of FXR ligands to increase NAGS transcription. Further on we observed that FXR activation directly stimulates urea production *in vivo* and *in vitro*. In conclusion, these data suggest a potential therapeutic role for FXR ligands in the treatment of hyperammonemia associated with liver diseases.

2. Material and methods

2.1. Isolation and culture of primary hepatocytes from FXR wild type and FXR deficient mice

Primary hepatocytes were isolated from C57BL6 wild type (Harlan Nossan) and FXR knockout animals (obtained from Gonzalez F.J. [15]) Briefly, mice were anesthetized with pentobarbital sodium solution (50 mg/kg i.p.), the inferior vena cava cannulated and the liver first perfused *in situ* with an oxygenated Hanks' buffer salt solution (HBSS) containing 100 U/mL penicillin/streptomycin (Invitrogen, Milan, Italy) and 0.04% collagenase-D (Roche, Milan, Italy) pH 7.4 (8 mL/min, 37 °C for 10 min), followed by perfusion with oxygenated HBSS containing 1 mM Ca_2^+ and Mg_2^+, penicillin/streptomycin (100 U/mL), and 0.04% collagenase II (Sigma, Milan, Italy), pH 7.4 for 10 min. The liver was removed and then gently minced in HBSS containing 1 mM Ca_2^+ and Mg_2^+, penicillin/streptomycin (100 U/mL), and 1×10^{-7} M insulin (Sigma, Milan, Italy) pH 7.4. The liver cell suspension was then filtered with Falcon cell strainers (40, 70, and 100 μm; Becton Dickinson, Milan, Italy) and centrifuged at $50\times g$ for 2 min. From the isolation of one mouse liver, a typical yield was about $50–60\times10^6$ hepatocytes. Cell viability, as determined by trypan blue exclusion, was generally >90%, and cell purity was >95% hepatocytes. Cells were plated on 6-well plates (6×10^5 cells/well) or 24-well plates (8×10^4) (Biocoat Collagen I cellware plates; Becton Dickinson, Milan, Italy) in William's Medium E (Invitrogen, Milan, Italy) containing 10% fetal bovine serum (Invitrogen, Milan, Italy), 100 U/mL penicillin/streptomycin, and 1×10^{-7} M insulin and cultured at 37 °C with 5% CO_2. After an initial 4-h attachment period, cultures were washed with phosphate-buffered saline (PBS) and then stimulated with CDCA (10 μmol/L) or with the synthetic FXR ligand GW-4064 (5 μmol/L) for 18 h. At the end of treatment RNA was extracted to value relative mRNA expression of ASCT1, ASCT2, EAAT2, NAGS, GDH, CPSI, GLS and GS by Real-Time PCR. To value urea synthesis primary hepatocytes were treated 18 h with NH_4Cl (10 mmol/L), GW-4064 (5 μmol/L), with the combination of NH_4Cl plus GW-4064 or with the combination of NH_4Cl plus N-acetylglutamate (5 mmol/L).

2.2. Animal studies

All animal procedures were approved by the Animal Study Committees of the University of Perugia. $FXR^{-/-}$ mice (obtained from Gonzalez F.J. [15]), and their backgrounds, C57BL/6j mice (Charles River Breeding Laboratories, Monza, Italy) were housed with a 12 h light/12 h dark cycle with free access to water and standard laboratory chow diet. Cirrhosis induced by carbon tetrachloride (CCl_4) was used as an experimental model of hyperammonemia. Cirrhosis was induced by administering phenobarbital sodium (35 mg/dL) into the drinking water for 3 days, followed by intraperitoneal injection (i.p.) of 100 μL/100 g body weight of CCl_4 in an equal volume of paraffin oil twice a week for 6 weeks. Mice administered CCl_4 were treated by i.p. of CDCA, 10 mg/kg body weight, while control animals were administered an equal volume of vehicle (methyl–cellulose). At the end of the study, mice were sacrificed and the livers removed to measure the relative mRNA expression of ASCT1, ASCT2, EAAT2, NAGS, GDH, CPSI, GLS and GS by Real-Time PCR. Blood samples were collected for plasma urea determination.

2.3. Urea and nitrogen assay

Urea concentration in plasma samples and culture mediums was measured by the QuantiChrom™ Urea Assay Kit (BioAssay Systems, Hayward, USA) according to the manufacturer's specifications. Serum levels of ammonium were measured by clinical chemistry testing performed on a Hitachi 717 automatic analyzer (Roche, Milan, Italy).

2.4. Determination of N-acetylglutamate (NAG) in mice liver tissues by HPLC–MS/MS

The amount of NAG in the livers of $FXR^{+/+}$ and $FXR^{-/-}$ mice was quantified in frozen tissues. 30 mg liver samples were homogenized with 400 μL of 2 M perchloric acid (PCA), sonicated and proteins were precipitated by centrifugation at 20,000 *g* for 10 min at 4 °C. The supernatants were neutralized with 400 μL of 2 M KOH/0.6 M MES solution. After centrifugation (20,000 *g*, 10 min, 4 °C), the supernatants were removed to glass vials and dried under N_2 stream. The obtained residues were taken up in a mix of 150 μL of distilled H_2O, 2% HCOOH and 0.05% TFA. An aliquot of 25 μL was injected into the HPLC–MS system LTQ XL ThermoScientific equipped with Accelera 600 Pump and Accelera AutoSampler system. The mixture was separated on a Jupiter 5μ C18 column from Phenomenex (150 × 2.00 mm) using as mobile phases H_2O—0.05% TFA—2% HCOOH (eluent A) and ACN—0.05% TFA—2% HCOOH (eluent B). The eluents were linearly changed from 0% B to 20% B within 10 min; the columns flow rate was set at 200 μL/min. The mass-spectrometer was set to operate with an ESI ionization source in positive mode. The capillary temperature was kept at 250 °C, the sheath gas flow rate and the auxiliary flow rate were set at 15 and 5, respectively. Instrument optimization was performed by direct infusion and manual tuning. Detection of NAG was performed using the selected reaction-monitoring mode (SRM). The transition of the NAG molecule to its corresponding product ions was recorded at m/z 190.2 → 131.2 ($-CH_3CONH_2$). The collision energy used was set at 35. Results are the mean ± SD of the value obtained for each independent animal in the respective group. (*$p<0.05$; **$p<0.001$)

2.5. Cell culture

HepG2 cells were grown at 37 °C in E-MEM containing 10% FBS, 1% L-glutamine and 1% penicillin/streptomycin. Cells were serum starved and treated 18 h with 10 μmol/L CDCA or 5 μmol/L GW4064. At the end of treatment RNA was extracted to value relative mRNA expression of ASCT1, ASCT2, EAAT2, NAGS, GDH, CPSI, GLS and GS by Real-Time PCR.

2.6. Real-Time PCR

Total RNA was isolated from cells or liver using the TRIzol reagent (Invitrogen, Milan, Italy), purified of the genomic DNA by DNase-I treatment (Invitrogen, Milan, Italy) and random reverse-transcribed with Superscript II enzyme (Invitrogen, Milan, Italy) according to the manufacturer's specifications. Fifty ng template was used in 25 μL final volume reaction of Real-Time PCR contained the following reagents: 0.2 μmol/L of each primer and 12.5 μL of 2X SYBR Green qPCR master mix (Invitrogen, Milan, Italy). All reactions were performed in triplicate and the thermal cycling conditions were: 2 min at 95 °C, followed by 40 cycles of 95 °C for 20 s, 55 °C for 20 s and 72 °C for 30 s in iCycler iQ instrument (BioRad, Milan, Italy). The results of Real-Time PCR were normalized with the housekeeping gene GAPDH and expressed as $2^{-(\Delta\Delta Ct)}$. All PCR primers were designed using software PRIMER3-OUTPUT using published sequence data from the NCBI database (Table 1).

2.7. Chromatin immunoprecipitation

10×10^6 HepG2 cells were stimulated 18 h with 10 μmol/L CDCA or received the vehicle alone (1% DMSO). At the end of the treatment cells were cross-linked with 1% formaldehyde at room temperature for 10 min. The reaction was terminated by incubation with glycine at the final concentration of 125 mM for 5′ at room temperature. Cells were lysed in 500 μL ChIP Lysis Buffer (1% SDS, 10 mmol/L EDTA, 50 mmol/L Tris–HCl pH 8), sonicated and then pelleted at 13,000 rpm 1′ at 4 °C. Supernatant was collected, diluted with ChIP dilution buffer (0.01% SDS, 1% Triton X-100, 1.2 mmol/L EDTA pH 8, 16.7 mmol/L Tris–HCl pH 8, 167 mmol/L NaCl) and 20 μg chromatin was immunoprecipitated with an anti-FXR antibody (H-130; Santa Cruz, CA, USA) or with an anti-IgG as negative control. Immunoprecipitates were collected with protein A beads (GE Healthcare, Milan, Italy) and washed sequentially, first with a low-salt wash buffer (0.1% SDS, 1% Triton X-100, 2 mmol/L EDTA pH 8, 20 mmol/L Tris–HCl pH 8, 150 mmol/L NaCl) and then with high-salt wash buffer (0.1% SDS, 1% Triton X-100, 2 mmol/L EDTA pH 8, 20 mmol/L Tris–HCl pH 8, 500 mmol/L NaCl). DNA was eluted with 500 μL Elution Buffer (1% SDS, 0.1 mol/L $NaHCO_3$) 30′ at 65 °C and the cross-linking reactions were reversed by adding 20 μL NaCL 5 mol/L and by heating the mixture overnight at 65 °C. The DNA was recovered from immunoprecipitated material by proteinase K treatment at 65 °C for 1 h followed by phenol/chloroform (1:1) extraction, ethanol precipitation and dissolved into 50 μL of water. Five microliters was used for quantitative real-time PCR of the NAGS promoter with the following forward and reverse primers: CACAGAATTCCTCAAGCTGG and CAGAGAAGAAGGGACTGTAG. Raw data analysis was performed as follows: ΔC_t was calculated *versus* the input DNA concentration; $\Delta\Delta C_t$ was *versus* unstimulated cells immunoprecipitated with the anti-IgG antibody (experimental condition set as 1.0); the relative expression was calculated as $2^{-(\Delta\Delta Ct)}$.

Table 1
Primers used for quantitative Real Time PCR analysis.

Gene	Forward	Reverse
Human GAPDH	gaaggtgaaggtcggagt	catgggtggaatcatattggaa
Human ASCT1	gcattctccaccacctgaat	gcgatgtctcctcctcagac
Human ASCT2	catcctgggcttggtagtgt	gatccaggagaccagaacca
Human EAAT2	cgccatctttatagcccaaa	cagaatgaggagcatggtga
Human NAGS	acaaaagaacggcagcagat	ggacccctgttgtcataaga
Human GDH	ggaggttcaccatggagcta	tggtgctggcataggtatca
Human CPSI	acatccagccgaattggtag	ctggagggttcagacagctc
Human GLS	ttccgaaagtgtgtgagcag	ccacaggtctgggtttgact
Human GS	tgatcctaagcccattcctg	tcataggcacggatgtggta
Mouse GAPDH	ctgagtatgtcgtggagtctac	gttggtggtgcaggatgcattg
Mouse ASCT1	gggaacgtgaccaaagagaa	ggcctcattgaaggaattga
Mouse ASCT2	caaccaaagaggtgctggat	cctccacctcacagagaagc
Mouse EAAT2	ggcaatcccaaactcaagaa	gtggtattggcctcctcaga
Mouse NAGS	cttcggagagacctgcaaac	ccgaaccagaagaagatcca
Mouse GDH	ggccgattgaccttcaaata	tcctgtcctggaactctgct
Mouse CPSI	aggcaccaccattacctcag	cgggttcatcaggactgttt
Mouse GLS	ccgtggtgaacctgctattt	tgcgggaatcatagtccttc
Mouse GS	cattgacaaactgagcaagagg	aagtcgttgatgttggaggttt

2.8. Electrophoretic mobility shift assay

Preparation of nuclear extract from HepG2 cells not treated or administered CDCA 10 μmol/L for 18 h was done using NE-PER (Pierce, Rockford, IL, USA). The probe used for EMSA (NAGS-ER8: TTTTGAGCTCAGGCAACAGGACAGAC) was labeled with biotin using Biotin 3′ end DNA labeling kit (Pierce, Rockford, IL, USA) according to the manufacturer's instructions. For EMSA, 10 μg of nuclear extract was incubated with 20 fmol of the NAGS-ER8 probe in a total volume of 20 μL of binding buffer (50 mmol/L NaCl, 10 mmol/L Tris–HCl, pH 7.9, 0.5 mmol/L EDTA, 10% glycerol, 1 μg of poly dI-dC) for 20 min at room temperature. For competition assays, an excess of NAGS-ER8 unlabeled oligonucleotide was pre-incubated with nuclear extract from CDCA-treated cells for 15 min prior to the addition of the biotin-labeled probe. For antibody-mediated supershift assay, extracts from stimulated cells were pre-incubated with 1 μg anti-FXR antibody (H-130; Santa Cruz, CA, USA) at room temperature for 15 min before the addition of the biotin-labeled probe. The reactions were loaded on a 6% polyacrylamide non-denaturing gel in 0.5 × Tris–borate–EDTA buffer and electrophoresed for 1 h at 100 V. The protein/DNA complexes were then transferred to positively charged nylon

membrane (Pierce, Rockford IL, USA), cross-linked at 120 mJ for 1 min and the supershift was detected using the Chemiluminescent Nucleic Acid Detection Module (Pierce, Rockford, IL, USA).

2.9. Plasmid construction, mutagenesis and luciferase assay

The human 5′ flanking region of NAGS gene, consisting of −558 to −332 base pairs with respect to the transcriptional start site ATG, was amplified by PCR from HepG2 genomic DNA (primers: atcgctcgagcacagaattcctcaagctggtacccagtga and cccgaagcttcagagaagaagggactgtaggtggctttga). PCR product was purified, double digested with Xho-I Hind-III enzymes and cloned into pGL3 promoter vector (Promega). The mutagenesis of ER8 responsive element was performed with the Quik change site directed mutagenesis kit (Stratagene). The primers used for the ER8 mutagenesis were the following: cattcattaggatctttttt**a**a**a**ctcaggcaacaggacagacaag and cttgtctgtcctgttgccygag**ttt**aaaaaagatcctaatgaatg. Primer sequences used for cloning three tandem repeats of the NAGS-ER8 wild type and mutated sequence into pGL3 promoter vector were the following: NAGS(ER8)$_{3X}$: atcgggtacctgagctcaggcaacaggacatgagctcaggcaacaggacatgagctcaggcaacaggacactcgagatcg and cgatctcgagtgtcctgttgcctgagctcatgtcctgttgcctgagctcatgtcctgttgcctgagctcaggtacccgat; NAGS(ER8mutated)3X: atcgggtacct**a**a**aa**tcaggcaacaggacat**a**a**aa**tcaggcaacaggggtacct**a**a**aa**tcaggcaacaggacat**a**a**aa**tcaggcaacaggt**a**a**aa**tcaggcaacaggacat**a**a**aa**tcaggcaacagg**a**a**aa**tcaggcaacaggacat**a**a**aa**tcaggcaacaggacat**a**a**aa**tcaggcaacaggacactcgagatcg and cgatctcgagtgtcctgttgcctga**ttt**atgtcctgttgcctga**ttt**atgtcctgttgcctga**ttt**ttatgtcctgttgcctga**ttt**atgtcctgttgcctga**ttt**aggtacccgat. These primers were oligo-annealed and the resulting double strand oligos were digested and cloned Kpn-I Xho-I into pGL3 promoter vector. For luciferase assay, cells were transfected with Fugene HD (Roche, Milan, Italy) Luminescence was measured with the Glomax 20/20 luminometer (Promega, Milan, Italy). Luciferase activities were normalized for transfection efficiencies by dividing the relative light units by β-galactosidase activity.

2.10. Western blot anti-NAGS

Total proteins extracted from liver specimens or cells were solubilized in NuPAGE sample buffer (Invitrogen) containing sample reducing agent (Invitrogen) and then separated by SDS PAGE. The proteins were then transferred to nitrocellulose membranes (Bio-Rad) and probed with primary antibodies NAGS (Abcam) and α-tubulin (Sigma). The anti-immunoglobulin G horseradish peroxidase conjugate (Bio-Rad) was used as the secondary antibody, and specific protein bands were visualized using Super Signal West Dura (Pierce), following the manufacturer's suggested protocol.

2.11. Statistical analysis

All values are expressed as mean ± SE of *n* observations per group. Comparisons of more than two groups were made with a one-way ANOVA with post-hoc Tukey's test. Differences were considered statistically significant if P was <0.05.

3. Results

3.1. FXR null mice have an impaired expression of genes involved in glutamine and glutamate transport and metabolism

We have first examined whether FXR gene ablation results in an altered expression of genes involved in glutamine and glutamate metabolism. Results from this experiment demonstrate that FXR gene ablation leads to a significant reduction in the expression of the glutamine transporter ASCT2, while the expression of the glutamate transporters, EAAT2 and ASCT1, were unchanged in FXR$^{-/-}$ mice in comparison with wild type mice. (Fig. 2A, n = 6; P<0.05). In addition, while the expression of GDH in FXR$^{-/-}$ livers was increased by approximately 3 folds in comparison with wild type mice (n = 6; P<0.05), the liver expression of NAGS, mRNA and protein, was reduced by ~40% (Fig. 2A and B, n = 6; P<0.05). No changes were found in the expression of CPSI, the enzyme mediating the first and limiting step of urea cycle, and GS, while the expression of GLS was slightly reduced in FXR$^{-/-}$ mice (Fig. 2A, n = 6; P<0.05). Because these changes predict that FXR gene ablation could result in an altered nitrogen balance, *i.e.* a reduced synthesis of urea, we have assessed blood levels of urea and ammonia in wild type and FXR$^{-/-}$ mice. Results shown in Fig. 2C and D demonstrate that at the age of 12 weeks, FXR$^{-/-}$ mice have a reduced plasma levels of urea and slight, but significant, increase of plasma ammonia levels (Fig. 2C and D, n = 6; P<0.05). These changes are in agreement with another investigation we made that in FXR$^{-/-}$ mice the production of NAG, the co-activator of CPSI, is basally reduced (Fig. 2E, n = 6; P<0.05).

3.2. FXR activation regulates the expression of genes involved in glutamine and glutamate transport and metabolism and enhances urea synthesis in primary mouse hepatocytes

We have next investigated the effects of natural and synthetic FXR agonists on genes involved in glutamate metabolism in hepatocytes isolated from FXR$^{+/+}$ and FXR$^{-/-}$ mice. As shown in Fig. 3A, treating FXR$^{+/+}$ hepatocytes with CDCA or GW-4064 resulted in a robust induction of mRNA expression of glutamine and glutamate transporters (ASCT1, ASCT2 and EAAT2) as well as of NAGS and GLS (n = 4; P<0.05). Furthermore, the expression of GDH mRNA was down-regulated following exposure to natural or synthetic FXR agonists (n = 4; P<0.05), while CPSI and GS mRNA were unchanged. By contrast, as shown in Fig. 3B, exposure of primary mouse hepatocytes isolated from FXR$^{-/-}$ mice to CDCA or GW-4064 failed to reproduce these changes. Because treatment of primary hepatocytes with NH_4Cl stimulates urea synthesis [16,17], we have investigated urea generation by FXR$^{+/+}$ and FXR$^{-/-}$ hepatocytes challenged with NH_4Cl in combination with an FXR agonist. As shown in Fig. 4A, production of urea in this setting was induced following exposure of FXR$^{+/+}$ hepatocytes to NH_4Cl. The synthetic FXR ligand GW-4064 was as effective as NH_4Cl in stimulating urea synthesis and the combination of two exerted an additive effect (Fig. 4; white bars, n = 4; P<0.05). By contrast, the urea production induced by both NH_4Cl, or GW-4064 or the combination of the two was markedly attenuated in FXR$^{-/-}$ hepatocytes (Fig. 4, black bars, n = 4, P<0.05) suggesting a role for FXR as regulator of the urea cycle. In order to evaluate whether the increased urea synthesis was really a consequence of increased NAGS expression we performed an experiment in FXR$^{+/+}$ and FXR$^{-/-}$ hepatocytes administered with NH_4Cl in presence of saturating amount of NAG. As shown in Fig. 4B, urea production was the same in these cells, indicating that induction of NAGS by FXR was crucial for stimulating urea synthesis. Similar data (*i.e.* RT-PCR results and urea determinations) were obtained using the HepG2 cells, a human hepatocytes cell line (Supplementary Fig. 1).

3.3. FXR activation restores the expression of genes involved in glutamine and glutamate metabolism in rodent model of liver cirrhosis

Since development of chronic liver failure is often associated with defects in glutamine/glutamate metabolism and urea cycle, which are the primary cause of hyperammonemia, we have investigated whether FXR plays a role in regulating *in vivo* metabolism of glutamine/glutamate in a model of hepatic damage induced in mice by CCl_4. Results shown in Supplementary Fig. 2, demonstrate that 6 weeks administration of CCl_4 induces liver cirrhosis as demonstrated by liver

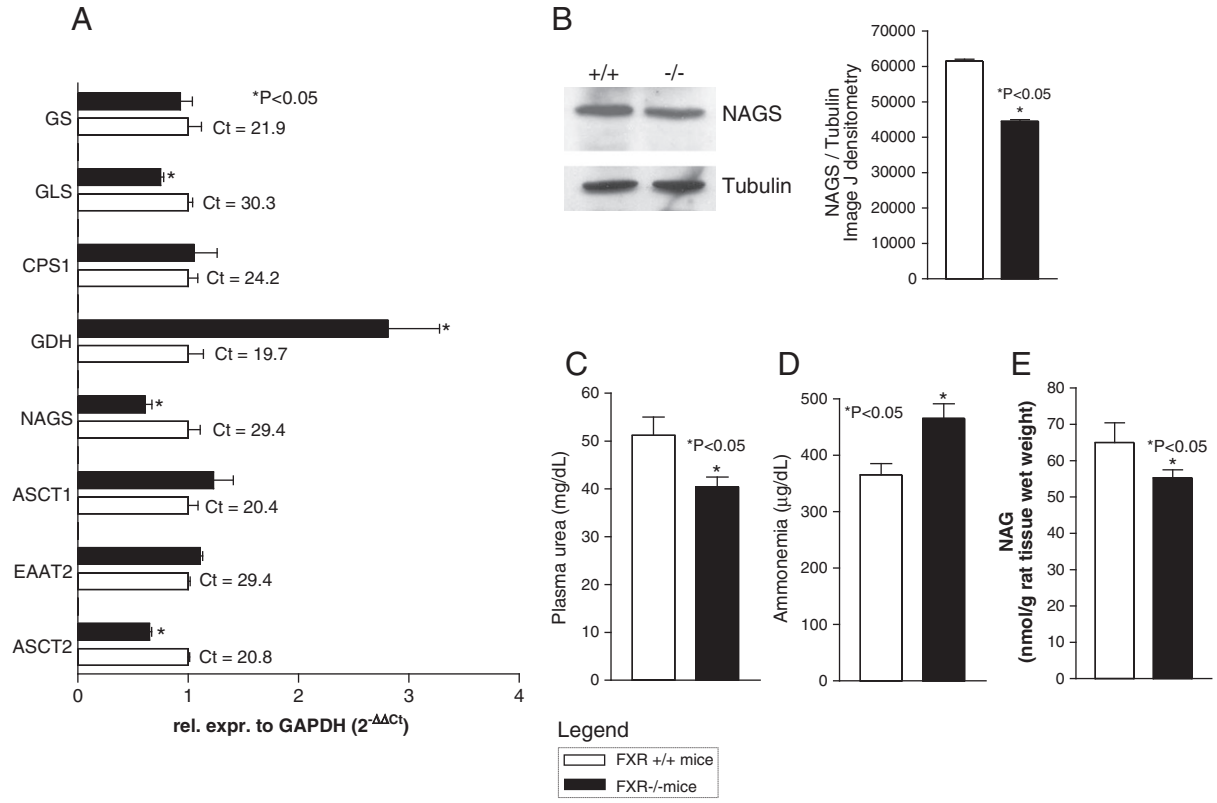

Fig. 2. FXR$^{-/-}$ mice have an altered expression of glutamine and glutamate metabolism genes and present a phenotype characterized by an impaired synthesis of urea and by an increased level of plasmatic ammonia. A, Liver mRNA from FXR$^{+/+}$ and FXR$^{-/-}$ mice was extracted to perform Real-Time PCR for ASCT2, EAAT2, ASCT1, NAGS, GDH, CPSI, GLS and GS. C_t mean values are referred to 100 ng cDNA template. B, Western blot analysis of NAGS expression in the liver. Liver homogenates from FXR$^{+/+}$ and FXR$^{-/-}$ mice were probed with an anti-NAGS or anti-tubulin as described in Material and methods. Quantitation was performed with Image J software. C, Plasma urea levels, D, plasma ammonia levels and E, liver amounts of N-acetylglutamate measured in FXR$^{+/+}$ and FXR$^{-/-}$ mice. Data shown are the mean ± SD of six mice per group. *P<0.05 *versus* FXR$^{+/+}$ mice.

histology and biochemical changes. Assessment of liver expression of genes involved in glutamine and glutamate metabolism in these mice demonstrates that histopathology features of liver cirrhosis associated with a significant reduction in the expression of EAAT2 and NAGS, with a significant induction of ASCT2 and GDH, while the expression of ASCT1, CPSI, GLS and GS was unchanged (Fig. 5A, n = 6, P<0.05). Treating mice

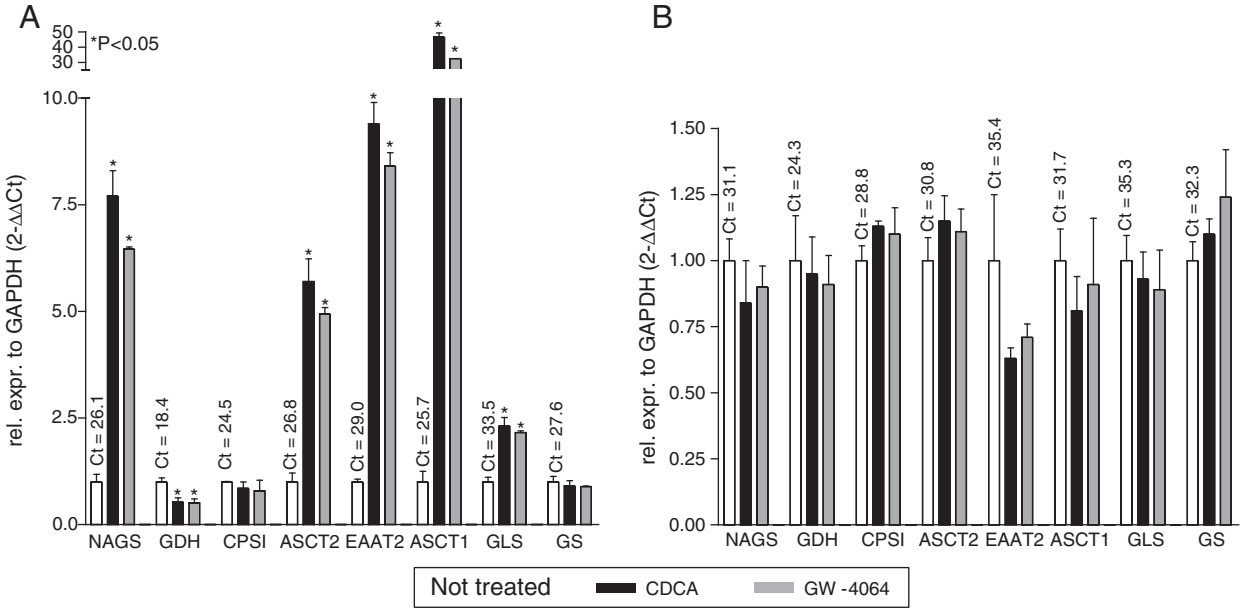

Fig. 3. FXR activation regulates glutamine and glutamate metabolism genes in primary hepatocytes isolated from FXR$^{+/+}$ mice but not in primary hepatocytes isolated from FXR$^{-/-}$ mice. A–B, Primary hepatocytes isolated from (A) FXR$^{+/+}$ mice or (B) FXR$^{-/-}$ mice were treated with CDCA (10 μmol/L) or GW-4064 (5 μmol/L) for 18 h. The relative mRNA expression of ASCT2, EAAT2, ASCT1, NAGS, GDH, CPSI, GLS and GS was calculated as described in Material and methods. C_t mean values are referred to 100 ng cDNA template. Data shown are the mean ± SD of four experiments. *P<0.05 *versus* not treated cells.

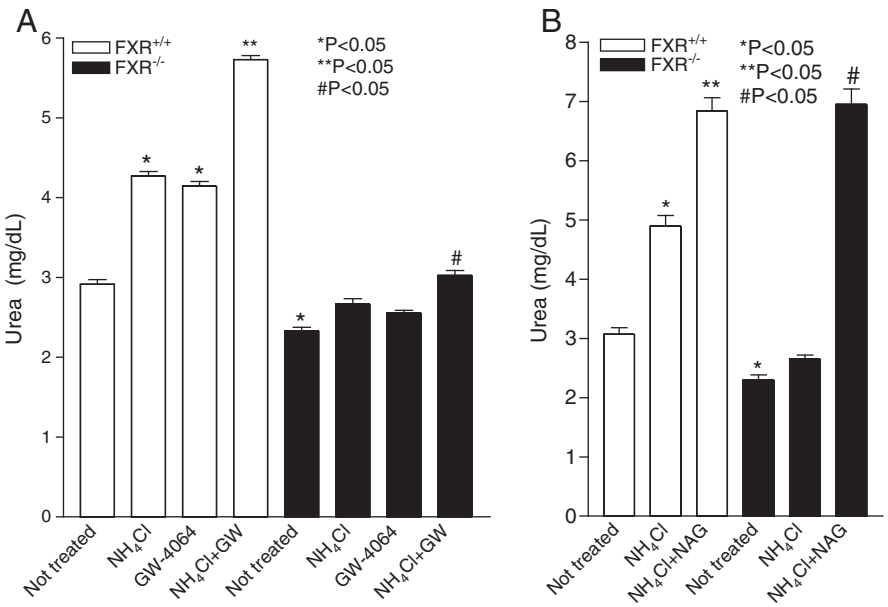

Fig. 4. Urea synthesis is impaired in $FXR^{-/-}$ hepatocytes and becomes equal to $FXR^{+/+}$ cells under saturating amounts of NAG. A, Primary hepatocytes isolated from $FXR^{+/+}$ mice (white bars) or $FXR^{-/-}$ mice (black bars) were treated with NH_4Cl (10 mmol/L) or GW-4064 (5 μmol/L) or with the combination of the two for 18 h. B, Primary hepatocytes isolated from $FXR^{+/+}$ mice (white bars) or $FXR^{-/-}$ mice (black bars) were treated with NH_4Cl (10 mmol/L) or with the combination of NH_4Cl (10 mmol/L) plus N-acetylglutamate (5 mmol/L) for 18 h. At the end of the treatments urea production was assayed in culture supernatants as described in Material and methods. Data shown are the mean ± SD of four experiments. *P<0.05 *versus* $FXR^{+/+}$ not treated cells; **P<0.05 *versus* $FXR^{+/+}$ cells treated with NH_4Cl; #P<0.05 *versus* $FXR^{-/-}$ cells treated with NH_4Cl.

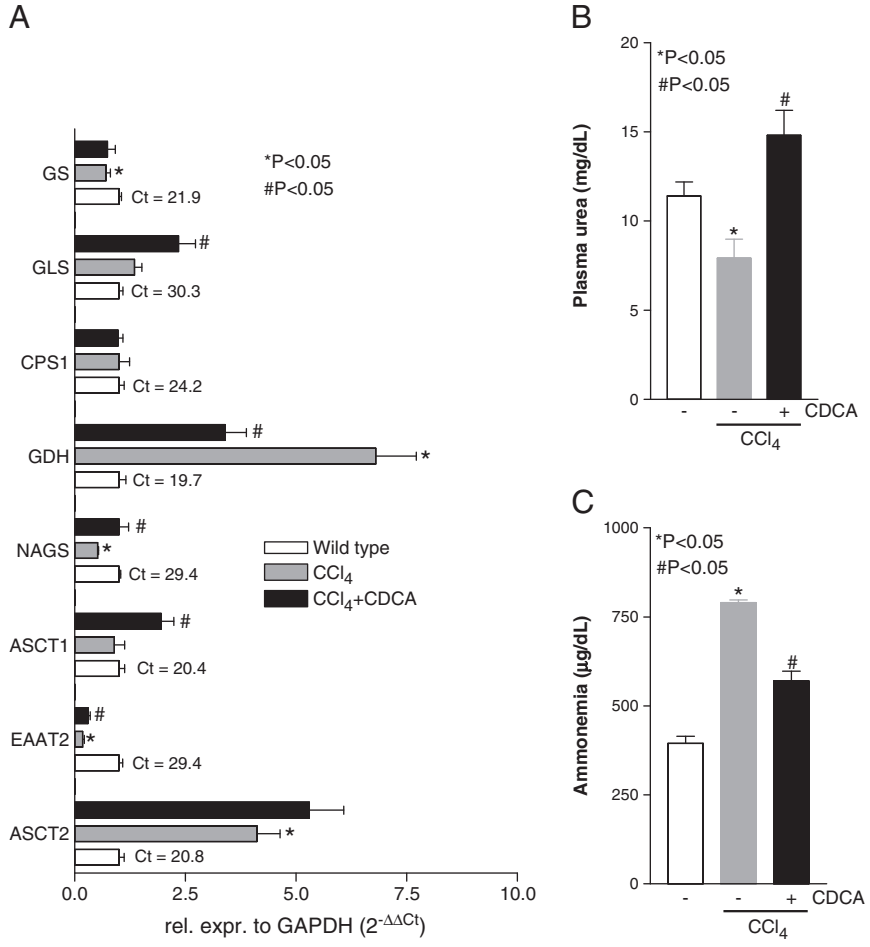

Fig. 5. FXR regulates the expression of genes involved in glutamine and glutamate metabolism in a model of liver cirrhosis induced by CCl_4 administration. Cirrhotic mice were administered with CDCA as described in Material and methods. A, Real-Time PCR analysis of liver expression of ASCT2, EAAT2, ASCT1, NAGS, GDH, CPSI, GLS and GS mRNAs. C_t mean values are referred to 100 ng cDNA template. B, Plasma levels of urea, and (C) plasma levels of ammonia in wild type, CCl_4 and CCl_4 administered CDCA mice. Data shown are the mean ± SD of six mice per group. *P<0.05 *versus* control mice; #P<0.05 *versus* CCl_4 administered mice.

Table 2
Promoter analysis of human and mouse 5′ flanking regions of glutamine and glutamate metabolism genes.

Gene (human)	Matrix: FXRE_38	Position with respect to the TSS	Score	Sequence
GS	Not found			
GLS (liver)	Not found			
NAGS	ER8	−476	0.73	TGAGCTcaggcaacAGGACA
GDH	ER-8	−564	0.61	TGAGCGccctacagAGGCCA
CPSI	Not found			
ASCT1	ER-8	−473	0.64	TGTCCCagaaagagAGGAAA
ASCT2	IR-1	−737	0.66	AGGTGAaTGACTT
EAAT2	Not found			
Gene (mouse)	**Matrix: FXRE_38**	**Position with respect to the TSS**	**Score**	**Sequence**
GS	IR-1	−132	0.66	CGGCCAaTGGCCT
GLS (liver)	ER-8	−974	0.66	TGGCCAcgaattcaAGGCCA
NAGS	ER-8	−593	0.68	TGACCTtgaactcgTGGATA
NAGS	ER-8	−41	0.65	TCACCTgtgggtggGGGGGA
GDH	Not found			
CPSI	Not found			
ASCT1	Not found			
ASCT2	Not found			
EAAT2	ER-8	−867	0.60	TGTCCCagtcctcgAGATAA

with CDCA resulted in an induction of the expression of ASCT1, EAAT2, NAGS and GLS as well as suppression of GDH mRNA (Fig. 5A, n = 6; P<0.05), while the expression of ASCT2, GS and CPSI was unaffected (Fig. 5A, n = 6, P<0.05). As illustrated in Fig. 5B and C, in comparison with naive animals, CCl_4-treated mice had significant lower plasma levels of urea but increased levels of ammonia. These biochemical abnormalities were corrected by treatment with CDCA (Fig. 5B and C, n = 6; P<0.05). All together these data illustrates that *in vivo* activation of FXR regulates the expression of genes involved in glutamine/glutamate metabolism and stimulates urea synthesis and ammonia detoxification in a rodent model of cirrhosis.

3.4. Identification and functional characterization of a putative FXRE in the NAGS promoter

Having shown that FXR regulates genes involved in glutamine/glutamate metabolism in tissues of murine and human origin, we have then searched for putative FXR responsive elements in the promoters of these genes. The NUBIScan analysis (http://www.nubiscan.unibas.ch) of the 5′ flanking regions (1000 base pairs upstream to the transcriptional start site — TSS) of human and mouse ASCT1, EAAT2, ASCT2, NAGS, GDH, CPSI, GLS and GS revealed the presence of putative FXR responsive sequences such as IR-1 and ER-8 in these promoters. However, only the NAGS gene has an FXRE conserved among the two species, an ER-8 sequence located at −476 base pairs with respect to the transcriptional start site ATG in the human NAGS promoter and at −593 base pairs in the murine promoter (Table 2). For practical reasons (*i.e.* ease of transfection, rapid replication and achievement of high number of cells to perform molecular experiments such as chromatin immunoprecipitation and EMSA) we have decided to assess the functionality of this ER-8 sequence in HepG2 cells instead of primary cultures of hepatocytes. To verify the hypothesis that FXR binds this ER-8 sequence, we have performed an EMSA experiment with a biotin-labeled ER-8 probe incubated with nuclear extracts obtained from HepG2 cells left untreated or primed with 50 μmol/L CDCA for 18 h. As shown in Fig. 6A this probe effectively binds nuclear extracts of unstimulated cells and CDCA treatment increased this interaction. We confirmed the specificity of this binding by adding 250 fold excess of unlabeled ER-8 probe or 1 μg FXR antibody. These approaches resulted in a complete abrogation of the binding of the ER-8 biotin labeled probe to the HepG2 nuclear extracts. Additionally, as shown in Fig. 6B, a ChIP assay conducted in serum-starved HepG2 cells exposed to CDCA demonstrated that FXR binds to a region in the NAGS promoter containing the above mentioned ER-8 sequence (n = 4; P<0.05).

The functional role of this interaction in regulating NAGS expression was further examined in transactivation experiments. First, a region

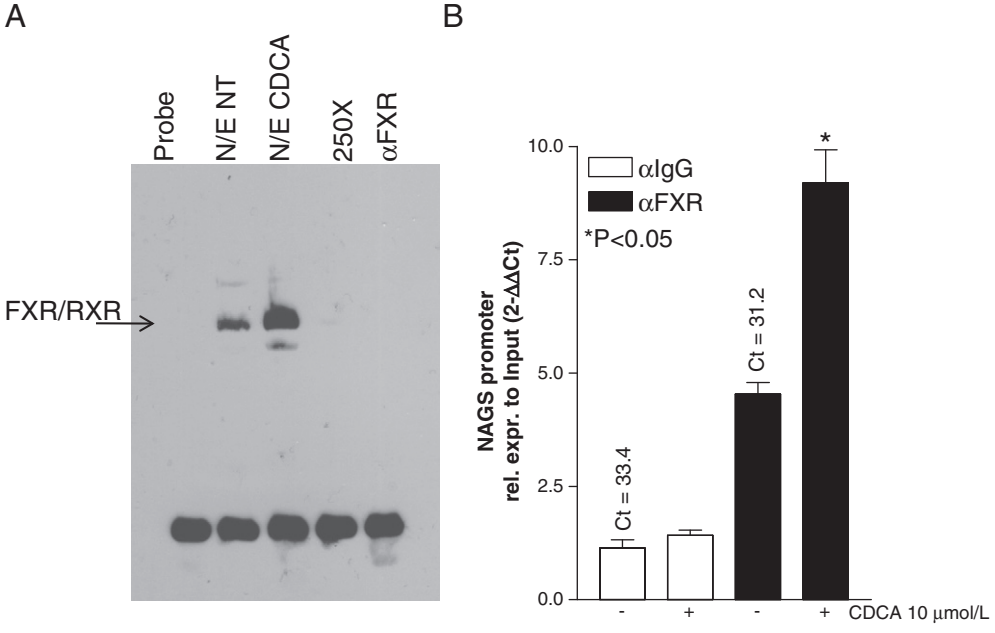

Fig. 6. FXR associates to the NAGS promoter. A, 3′ Biotin labeled oligonucleotide NAGS FXRE ER8 was incubated with or without nuclear extracts (N/E) from HepG2 cells not treated (NT) or stimulated with CDCA 10 μmol/L. After incubations an electrophoretic run was performed as follows: lane 1: probe alone; lane 2: probe plus N/E of untreated cells; lane 3: probe plus N/E of stimulated cells. Competition experiments were performed with an excess of unlabeled oligo (lane 4) or with 1 μg FXR antibody (lane 5). B, ChIP assay carried out in HepG2 cells left untreated or primed with 10 μmol/L CDCA. This experiment confirms that FXR binds the ER-8 sequence in the context of intact chromatin. ΔC_t was calculated *versus* the input DNA concentration; $\Delta\Delta C_t$ was *versus* unstimulated cells immunoprecipitated with the anti-IgG antibody; the relative expression was calculated as $2^{-(\Delta\Delta Ct)}$. C_t values are referred to 5 μL chromatin. Data shown are the mean ± SD of four experiments. *P<0.05 *versus* not treated cells.

of the human NAGS promoter containing the ER-8 sequence (−558/−332) was amplified by PCR and cloned into a pGL3 promoter vector. Using this reporter vector we have transfected HepG2 cells with different concentrations of the plasmid pSG5-FXR (50, 100 and 200 ng) in the presence of the heterodimeric partner RXR. As shown in Fig. 7A, transient transfection assays revealed a dose-dependent activation of the NAGS promoter (Fig. 7A, n = 4, $P<0.05$). As expected, the mutagenesis of the ER8 sequence in the context of the NAGS promoter prevented its activation by FXR (Fig. 7B). In order to confirm these results, we have cloned three copies of the NAGS ER-8 sequence or three copies of the mutated ER-8 (TGTTCT*caggcaac*ATTACA) into a pGL3 promoter vector ($pGL3(ER8)_{3X}$ or a $pGL3(ER8mut)_{3X}$). Using these reagents we have carried out luciferase experiments in HepG2 cells transfected with pSG5-FXR and pSG5-RXR expression vectors and then treated with CDCA (10 μmol/L) or GW4064 (5 μmol/L) for 18 h. As shown in Fig. 7C, in the presence of the luciferase reporter containing three repeats of the wild type sequence ER-8, cotransfection with FXR and RXR, *per se* was able to induce an ≈2 fold increase in the luciferase activity (Fig. 7C, n = 4, column 1 *versus* 2, $P<0.05$) and the treatment with the natural or synthetic FXR ligand resulted in an ≈3/4 fold increase in luciferase activity (column 1 *versus* 3 and 4, $P<0.05$). By contrast, when HepG2 cells were transfected with pSG5-FXR and pSG5-RXR expression vectors in the presence of the luciferase reporter containing three tandem repeats of the ER-8 mutated sequence the transactivation of FXR was completely abrogated in both unstimulated and stimulated conditions (Fig. 7D, n = 4). Overall, these results demonstrated that the response element ER-8 in the NAGS promoter is crucial for the FXR dependent induction of NAGS.

4. Discussion

Chronic liver disorders are traditionally characterized by an impaired liver function caused by various factors such as nodular regeneration of hepatocytes, altered expression of genes involved in glutamine and glutamate metabolism, altered liver perfusion contributed by porto-systemic shunting, and progressive disturbance of liver urea metabolism leading to accumulation of ammonia in the blood and tissues. [18–20]. The molecular mechanisms that lead to

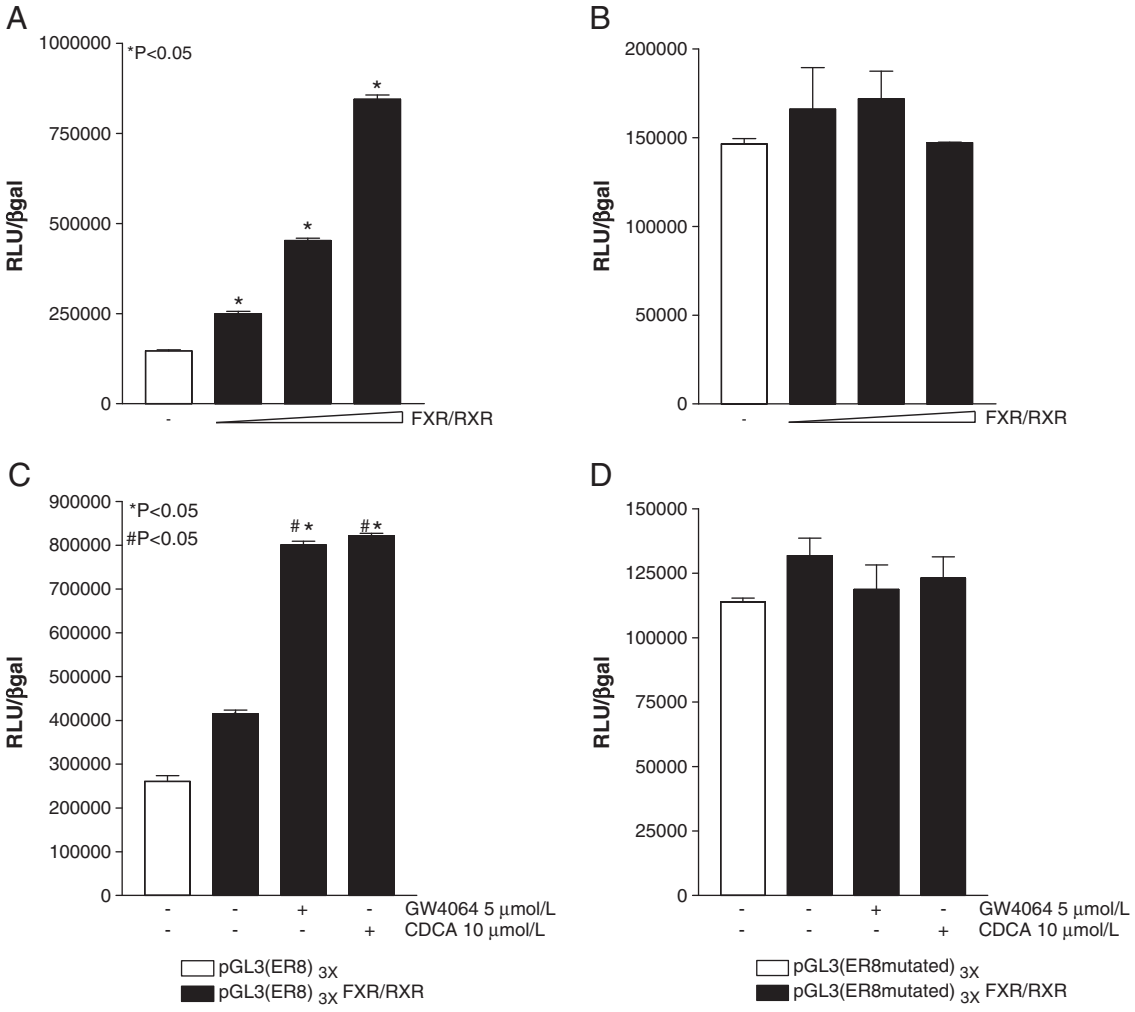

Fig. 7. Promoter activation of the NAGS is regulated by FXR. A, Luciferase activity of the human NAGS 5′flanking region (−558/−332) in HepG2 cells not trasfected or trasfected with 50, 100 and 200 ng of pSG5-FXR and pSG5-RXR. Data shown are the mean ± SD of four experiments. *$P<0.05$ *versus* pGL3(−558/−332)NAGS trasfected cells. B, Luciferase activity of the human NAGS promoter (−558/−332) containing the ER8 mutated sequence. HepG2 cells not trasfected or trasfected with 50, 100 and 200 ng of pSG5-FXR and pSG5-RXR were used. Data are the mean ± SD of four experiments. C, Three tandem repeats of the ER-8 sequence were cloned into pGL3 vector. HepG2 cells were transfected with the pGL3(ER8)3x and pCMV-βgalactosidase vector alone or in combination with pSG5-FXR and pSG5-RXR vectors. 24 hours post transfection cells were stimulated with 10 μmol/L CDCA or with 5 μmol/L GW4064 for 18 h. Luciferase activity is shown as the ratio of luciferase to β-galactosidase activities. Data are the mean ± SD of four experiments. *$P<0.05$ *versus* pGL3 $(ER8)_{3x}$ transfected cells; #$P<0.05$ *versus* cells transfected with $pGL3(ER8)_{3x}$ plus FXR and RXR expressing vectors. D, Three tandem repeats of the ER-8 mutated sequence were cloned into pGL3 vector. HepG2 were transfected with pGL3(ER8mut)3x and pCMV-βgalactosidase alone or in combination pSG5FXR and pSG5-RXR. 24 hours post transfection cells were stimulated with 10 μmol/L CDCA or with 5 μmol/L GW4064 for 18 h. Luciferase activity is shown as the ratio of luciferase to β-galactosidase activities. Data shown are the mean ± SD of four experiments.

altered hyperammonia in chronic liver disease are not completely understood.

In the present study we provide compelling evidence for a regulatory role of bile acids on glutamine/glutamate metabolism and urea detoxification by activation of the nuclear receptor FXR.

Support to this notion comes from the observation that mice harboring a disrupted FXR gene develop hyperammonemia in association with reduced blood levels of urea. This phenotype associates with an altered liver expression of genes encoding for proteins involved in glutamine and glutamate metabolism. Thus, we found that while the expression of glutamine transporter ASCT2, glutaminase and NAGS was significantly downregulated in the liver of $FXR^{-/-}$ mice, the expression of the glutamate transporter EAAT2, ASCT1 and CPSI and glutamine synthase was unchanged in $FXR^{-/-}$ mice with respect to the wild type strain. By contrast, the relative expression of GDH mRNA was induced by ≈3 fold. Overall these data confirmed that depletion of FXR *in vivo* suffices *per se* to drive an altered expression of genes involved in glutamine and glutamate metabolism and confirmed previous studies establishing that the glutamine transporter ASCT2 is directly regulated by the activation of FXR [14]. Support to this view comes also from the finding that *ex vivo* treatment of primary mouse hepatocytes isolated from $FXR^{+/+}$ mice with CDCA or GW-4064 regulates the expression of genes involved in glutamine and glutamate metabolism and enhances the urea synthesis in these cells. Importantly, these regulatory effects were completely lost in primary hepatocytes isolated from $FXR^{-/-}$ mice, strongly indicating an essential role for FXR in mediating adaptive changes of these genes in response to bile acids. Similar results were obtained using HepG2 cells stimulated with CDCA or GW-4064.

Since these data suggest that FXR exerts a regulatory role on genes involved in glutamine and glutamate metabolism – assuming the use of FXR ligands in the treatment of ammonia disorders – we have next investigated whether the expression of genes involved in glutamine and glutamate metabolism is modulated in a rodent model of liver cirrhosis. The results of these experiments confirmed that the development of hyperammonemia in CCl_4 mice associates with a reduction of blood urea concentrations along with a severe reduction in the liver expression of NAGS and EAAT2 mRNA. By contrast, the relative mRNA expression of ASCT2 and GDH appeared induced while the mRNA expression of ASCT1, CPSI, GLS and GS was apparently unchanged in CCl_4 mice. Importantly, we found that the levels of NAGS, ASCT1, EAAT2, GLS and GDH were regulated by treating mice with an FXR ligand. Indeed, EAAT2, ASCT1, NAGS and GLS were induced while GDH was downregulated in CCl_4 mice administered with an FXR ligand. Overall, the regulation of these genes by CDCA associates with an increased synthesis of urea and a restored ammonia detoxification in cirrhotic mice.

Deficiency of N-acetylglutamate is the most severe of the urea cycle disorders [21,22] leading to severe reduction of the CPS-I activity, the first enzyme, and limiting step, of urea cycle. Indeed, deficiency of CPS-I impairs conversion of ammonia into carbamyl phosphate, blocking the synthesis of urea. In noncirrhotic settings, NAGS deficiency is biochemically characterized by an increased level of plasmatic ammonia, whereas the concentration of other urea-cycle intermediates is low or normal [21,22]. The majority of patients with NAGS deficiency caused by frameshift or nonsense mutations have <5% residual activity [23–25]. Complete NAGS deficiency leads to hyperammonemia in the newborn period and subjects that are successfully rescued from crisis are chronically at risk for repeated bouts of hyperammonemia [23–25]. It has been recently demonstrated that derivatives of L-glutamic acid, in particular, N-carbamylglutamate could activate the biosynthesis of carbamyl phosphate by CPS-I, thus restoring, at least partially, the synthesis of urea in patients with NAGS deficiency [26,27].

In the present study we have demonstrated that the FXR/RXR heterodimer binds specifically to an ER8 sequence located at −476 bp from the transcriptional start site ATG in the human NAGS promoter. The characterization of the functionality of this ER8 was obtained by both gel mobility shift and ChIP assay. Further on, mutagenesis experiments demonstrated that the FXR/RXR heterodimer becomes unable to induce luciferase activity when this ER8 sequence was mutated. In aggregate, these data established that NAGS is an FXR regulated gene and that regulation of expression of this gene by FXR is mediated *via* activation of an ER8 sequence. All together these molecular data are of clinical relevance because an inducer of NAGS might hold utility in the treatment of hyperammonia in chronic liver disorders. The identification of NAGS as direct FXR targets is consistent with results of genome wide analysis indicating that approximately 25% of genes involved in amino acid and nitrogen metabolism are potential targets for FXR [28].

In conclusion, the present study describes for the first time that FXR activation regulates genes involved in the glutamine and glutamate metabolism (*i.e.* genes involved in the glutamine and glutamate uptake, conversion of glutamine into glutamate and glutamate into NAG) and enhances urea synthesis in hepatocytes. Thus, activation of FXR could be beneficial for the treatment of hyperammonemia in chronic liver diseases.

Appendix A. Supplementary data

Supplementary data to this article can be found online at doi:10.1016/j.bbadis.2011.06.009.

References

[1] D. Yang, H. Brunengraber, Glutamate, a window on liver intermediary metabolism, J. Nutr. 130 (4S Suppl.) (2000) 4S–991.
[2] M. Watford, Glutamine and glutamate metabolism across the liver sinusoid, J. Nutr. 130 (4S Suppl.) (2000) 7S–983.
[3] A. Braeuning, C. Ittrich, C. Köhle, S. Hailfinger, M. Bonin, A. Buchmann, et al., Differential gene expression in periportal and perivenous mouse hepatocytes, FEBS J. 273 (22) (2006) 5051–5061.
[4] M.E. Brosnan, J.T. Brosnan, Hepatic glutamate metabolism: a tale of 2 hepatocytes, Am. J. Clin. Nutr. 90 (3) (2009) 61S–857S.
[5] H. Morizono, L. Caldovic, D. Shi, M. Tuchman, Mammalian N-acetylglutamate synthase, Mol. Genet. Metab. (Suppl. 1) (2004) S4–S11.
[6] A. Plaitakis, I. Zaganas, Regulation of human glutamate dehydrogenases: implications for glutamate, ammonia and energy metabolism in brain, J. Neurosci. Res. 66 (5) (2001) 899–908.
[7] P.M. Beart, R.D. O'Shea, Transporters for L-glutamate: an update on their molecular pharmacology and pathological involvement, Br. J. Pharmacol. 150 (1) (2007) 5–17.
[8] S. Fiorucci, A. Mencarelli, E. Distrutti, G. Palladino, S. Cipriani, Targetting farnesoid-X-receptor: from medicinal chemistry to disease treatment, Curr. Med. Chem. 17 (2) (2010) 139–159.
[9] M. Trauner, T. Claudel, P. Fickert, T. Moustafa, M. Wagner, Bile acids as regulators of hepatic lipid and glucose metabolism, Dig. Dis. 28 (1) (2010) 220–224.
[10] S. Fiorucci, A. Mencarelli, G. Palladino, S. Cipriani, Bile-acid-activated receptors: targeting TGR5 and farnesoid-X-receptor in lipid and glucose disorders, Trends Pharmacol. Sci. 30 (11) (2009) 570–580.
[11] B. Renga, A. Mencarelli, P. Vavassori, V. Brancaleone, S. Fiorucci, The bile acid sensor FXR regulates insulin transcription and secretion, Biochim. Biophys. Acta 1802 (3) (2010) 363–372.
[12] S. Fiorucci, S. Cipriani, A. Mencarelli, B. Renga, E. Distrutti, F. Baldelli, Counter-regulatory role of bile acid activated receptors in immunity and inflammation, Curr. Mol. Med. 10 (6) (2010) 579–595.
[13] P.A. Edwards, H.R. Kast, A.M. Anisfeld, BAREing it all: the adoption of LXR and FXR and their roles in lipid homeostasis, J. Lipid Res. 43 (1) (2002) 2–12.
[14] C.I. Bungard, J.D. McGivan, Identification of the promoter elements involved in the stimulation of ASCT2 expression by glutamine availability in HepG2 cells and the probable involvement of FXR/RXR dimers, Arch. Biochem. Biophys. 443 (1–2) (2005) 53–59.
[15] C.J. Sinal, M. Tohkin, M. Miyata, J.M. Ward, G. Lambert, F.J. Gonzalez, Targeted disruption of the nuclear receptor FXR/BAR impairs bile acid and lipid homeostasis, Cell 102 (2000) 731–744.
[16] T. Mutsvangwa, J.G. Buchanan-Smith, B.W. McBride, Effects of ruminally degradable nitrogen intake and in vitro addition of ammonia and propionate on the metabolic fate of L-[1-14C]alanine and L-[15N]alanine in isolated sheep hepatocytes, J. Anim. Sci. 75 (4) (1997) 1149–1159.
[17] Y. Ohtake, M.G. Clemens, Interrelationship between hepatic ureagenesis and gluconeogenesis in early sepsis, Am. J. Physiol. 260 (3 Pt 1) (1991) E453–E458.
[18] S.W. Brusilow, N.E. Maestri, Urea cycle disorders: diagnosis, pathophysiology, and therapy, Adv. Pediatr. 43 (1996) 127–170.
[19] R. Jalan, D. Shawcross, N. Davies, The molecular pathogenesis of hepatic encephalopathy, Int. J. Biochem. Cell Biol. 35 (2003) 1175–1181.

[20] O. Braissant, Current concepts in the pathogenesis of urea cycle disorders, Mol. Genet. Metab. 100 (Suppl 1) (2010) S3–S12.
[21] J.P. Colombo, N-acetylglutamate synthetase (NAGS) deficiency, Adv. Exp. Med. Biol. 368 (1994) 135–143.
[22] L. Caldovic, N. Ah Mew, D. Shi, H. Morizono, M. Yudkoff, M. Tuchman, N-acetylglutamate synthase: structure, function and defects, Mol. Genet. Metab. 100 (Suppl. 1) (2010) S13–S19.
[23] L. Caldovic, H. Morizono, M. Tuchman, Mutations and polymorphisms in the human N-acetylglutamate synthase (NAGS) gene, Hum. Mutat. 28 (2007) 754–759.
[24] C. Bachmann, J.P. Colombo, K. Jaggi, N-acetylglutamate synthetase (NAGS) deficiency: diagnosis, clinical observations and treatment, Adv. Exp. Med. Biol. 153 (1982) 39–45.
[25] J. Haberle, E. Schmidt, S. Pauli, J.G. Kreuder, B. Plecko, A. Galler, et al., Mutation analysis in patients with N-acetylglutamate synthase deficiency, Hum. Mutat. 21 (2003) 593–597.
[26] J. Hinnie, J.P. Colombo, B. Wermuth, F.J. Dryburgh, N-acetylglutamate synthetase deficiency responding to carbamylglutamate, J. Inherit. Metab. Dis. 20 (1997) 839–840.
[27] A.A. Morris, S.W. Richmond, S.J. Oddie, M. Pourfarzam, V. Worthington, J.V. Leonard, N-acetylglutamate synthetase deficiency: favourable experience with carbamylglutamate, J. Inherit. Metab. Dis. 21 (1998) 867–868.
[28] A.M. Thomas, S.N. Hart, B. Kong, J. Fang, X.B. Zhong, G.L. Guo, Genome-wide tissue-specific farnesoid X receptor binding in mouse liver and intestine, Hepatology 51 (4) (2010) 1410–1419.